



**Research Article**

**BEHAVIOR OF RC BUILDING WITH AND WITHOUT INFILL WALL  
UNDER BLAST LOADING**

**Sabiou NAMATA SAIDOU\*<sup>1</sup>, Ali KOÇAK<sup>2</sup>**

<sup>1</sup>*Yildiz Technical University, Civil Engineering Dept., Esenler-ISTANBUL; ORCID:0000-0001-6655-8814*

<sup>2</sup>*Yildiz Technical University, Civil Engineering Dept., Esenler-ISTANBUL; ORCID:0000-0002-5874-2715*

**Received: 18.01.2018 Revised: 30.04.2018 Accepted: 25.07.2018**

**ABSTRACT**

In this work the authors intended to improve the knowledge regarding to RC and masonry structures subjected to blast loading. A further aim is to describe and use the non-linear-finite element method through a comparison of RC building with and without infill wall.

In order to perform the models subjected to analysis, based on existing experimental studies of infill wall and RC columns, by using the FE method, the blast loading is simulated using conventional weapons for explosion model where it was generated with 1000kg of TNT explosive material at a distance of 4.6m.

For the finite element model of the building, bricks and mortar joints are represented by continuously cohesive elements and contact elements were used to simulate the adhesion and interaction between the blocks. The nonlinear behavior of the concrete and masonry were simulated using the Coupled Damage Plasticity methods. Simulation results showed that compressive and tensile strengths increase due to the strain rate effect and the initial stiffness increases.

**Keywords:** Building, infill wall, blast, masonry, finite element.

**1. INTRODUCTION**

Blast loading has received more attention in recent years because of accidental and intentional events (terrorist attacks) that affected important structures. In particular during the last decade the development of building and structure vulnerability under blast loading occurred extensively. To find out solution about the phenomena of blast resistance of structures, a number of analytical and numerical researches have been done and published in the international literature using software's for scientific and engineering designs.

The analysis and design of structures subjected to blast loads require a detailed understanding of blast phenomena and the dynamic response of various structural elements. Due to the high cost, it is almost impossible to investigate the response of multi-storey buildings against blast loads, with full-scale experimental tests.

However, most of the current numerical modeling research is involved with massive computational time and the model is difficult to build due to its complexity. Therefore, for designers, it is imperative to establish a simple modeling method to study the detailed behavior of

\* Corresponding Author: e-mail: namata.saidou@std.yildiz.edu.tr, tel: (212) 383 52 17

the building after the blast denotation. Techniques developed by Feng Fu [1], with ABAQUS, a 3-D finite element model representing a 20-storey building was built to perform the blast analysis, a simulation method of blast load is applied, the nonlinear material behavior and dynamic effects are also included in the simulation.

The blast effect on a building can also affect its environment, in this same order of idea, Alex et al. [2], provided an accurate prediction of the effects of adjacent structures on the blast loads on a building in urban terrain. In the paper, an attempt has been made to characterize the blast environment by considering a simple urban configuration with a relatively long, straight street segment and a T-junction at the far end. Numerical simulations using a computational Fluid dynamics (CFD) code Air3D has been used to determine the blast effects on the building in a typical urban terrain. Each simulation provided the variation with distance of peak overpressure and impulse. When compared with the corresponding variations for a surface burst of hemispherical charge in free-field environment, these variations in the calculation of the pressure and impulse enhancement factors at each scaled distance from the charge. The resulting enhancement factors effectively modify the blast parameters obtained from simplified analytical techniques.

## 2. BLAST LOADING

### 2.1. Prediction of Blast Pressure

Blast wave parameters for conventional high explosive materials have been the focus of a number of studies during 1950's and 1960's. Estimations of peak overpressure due to spherical blast loading, based on scaled distance  $Z = R/W^{1/3}$  was introduced by Brode (1955) as:

$$P_{so} = \frac{6.7}{Z^3} + 1bar(P_{so}) \tag{1}$$

$$P_{so} = \frac{0.975}{Z} + \frac{1.455}{Z^2} + \frac{5.85}{Z^3} - 0.019 \text{ bar} \tag{2}$$

$$0.1 < P_{so} < 10 \text{ bar}$$

Newmark and Hansen (1961) introduced relationship to calculate the maximum blast overpressure,  $P_{so}$ , in bars, for a high explosive charge detonates at the ground surface as:

$$P_{so} = 6784 \frac{W}{R^3} + 93 \left( \frac{W}{R^3} \right)^{1/2} \tag{3}$$

Another expression of the peak overpressure in kPa is introduced by Mills (1987), in which  $W$  is expressed as the equivalent charge weight in kilograms of TNT and  $Z$  is the scaled distance, as follow:

$$P_{so} = \frac{1772}{Z^3} - \frac{114}{Z^2} + \frac{108}{Z} \tag{4}$$

### 2.2. Simulation of Explosion Effect on the Air

According to ConWep model, the pressure exerted on a structure's surface caused by the blast wave is function of incident pressure  $P_{incident}$  (t), reflected pressure  $P_{reflect}$  and Angle of incidence  $\theta$ . Pressure is defined by Mourizt [3] as:

$$\begin{cases} P(t) = P_{incident}(t) [1 + \cos \theta - 2 \cos^2 \theta] + P_{reflect}(t) \cos^2 \theta, & \cos \theta > 0 \\ P(t) = P_{incident}(t), & \cos \theta < 0 \end{cases} \quad (5)$$

### 3. MODELING OF EXPERIMENTAL STUDIES

#### 3.1. Model I: Infill Wall Model

##### 3.1.1. Test Setup

The tested wall consisted, of 3.5 x 1.7 m2 masonry panel of 150 mm of hollow clay block and 15 mm with plaster on each side, Figure 1. To hold the wall, a reinforced concrete frame with 180 mm of thickness and steel diagonal with frame elements were used to keep the frame smooth.

A large water tank (1 meter cubic) is placed on one side of the wall to operate as blast wave generator (BWGs) which consisted in application of the desired load. The pressure rises to 149 kPa in the first 6 ms, then decays and reaches 119 kPa at 17.5 ms and stops acting after 29 ms.

On the other side of the wall, measuring devices were installed to obtain the desire behavior of the wall. The maximum deviation was measured using the laser and high-speed video equipment which was used to examine the behavior of the wall during test. To provide safety and protection during the test, test site was surrounded with walls and some safe area which provided good accommodation of the equipment.

The wall specimen was previously tested in different conditions and additional details on the composition and construction procedure of this sample are included in Pereira et al. [3] and [5].

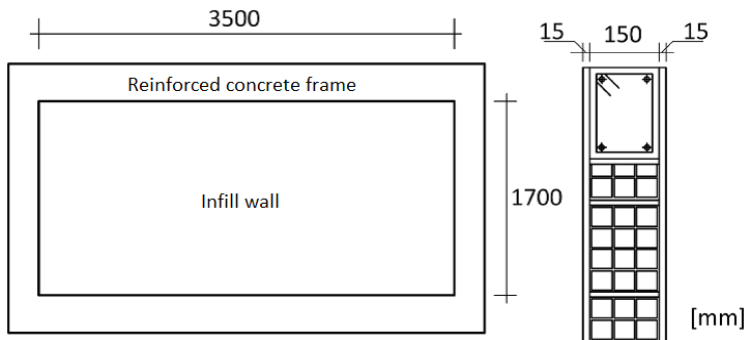


**Figure 1.** Infill wall model

The numerical model of infill wall consisted of blocks and mortar in which elements are interconnected by a three-dimensional solid eight node elements (C3D8R). To establish connections between mortar and blocks, COH2D4 elements with two integrator nodes were used and elements sizes were selected after studying mesh dependence. The modified Drucker-Prager flow potential hypothesis was accepted and Concrete Damaged Plasticity (CDP) material model has been used. The CDP model is characterized by the damage plasticity of material both under stress cracking and pressure, where the isotropic stress and pressure plasticity to represent the inelastic and fracture behavior of the material it required the definition of the following five parameters:

- expansion angle ( $\Psi$ ); is the dilation angle measured in the p-q plane at high confining Pressure;
- flow eccentricity ( $\epsilon$ ); is an eccentricity of the plastic potential surface;

- the ratio of initial equibiaxial compressive yield stress to initial uniaxial compressive yield stress ( $f_{bo}/f_{co}$ );
- viscosity parameter ( $\mu$ );
- Parameter  $K$ .

The parameters  $\Psi$  and  $\varepsilon$  are used to describe the shape of the flow potential function, while  $f_{bo}/f_{co}$  and  $K$  are responsible for the shape of the yield function. For the identification of these parameters, laboratory tests are necessary but in this paper the same default values used by Pereira et. al. [6] has been used as shown in the Table 1.

**Table 1.** CDP model parameters

$\Psi$	$\varepsilon$	$f_{bo}/f_{co}$	$\mu$	$Kc$
$40^\circ$	0.1	1.16	0.0	0.667

Mechanical properties of the masonry and stress-strain relations curves (Figure 2) are shown as follow:

- The density of the concrete brick unit has been assumed as 1800 kg/m<sup>3</sup>.
- Young’s modulus  $E = 3.6 \times 10^{10}$  Pa.
- Poisson’s ratio  $\nu = 0.2$ .
- Compressive Strength = 1.26 MPa
- Tensile Strength=0.125 MPa and the Mode I fracture energy=0.012[N/mm]

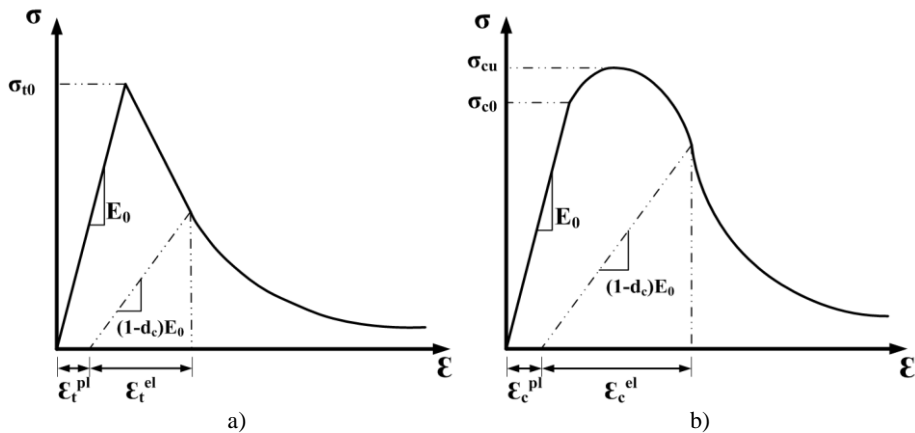


**Figure 2.** Stress-strain relations: a) Tensile; b) Compression [6].

### 3.1.2. Results

Experimental and numerical curves of the maximum displacement at midpoint of the wall have been compared as shown in the Figure 3. It’s clearly observed that the two curves are almost identical, thus the model can be validated.

The maximum principal plastic strain values were plotted in Figure 4. As expected the maximum damage is located in the central, top and bottom area of the masonry wall. This result is in a good accordance with the experimental result.

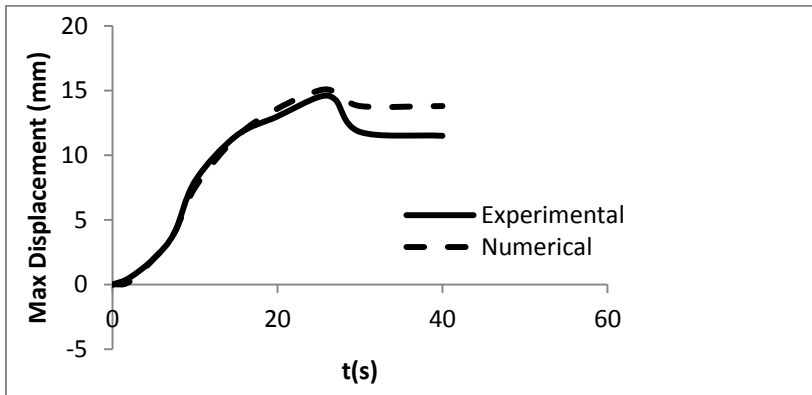


Figure 3. Comparison between numerical and experimental results, [5].

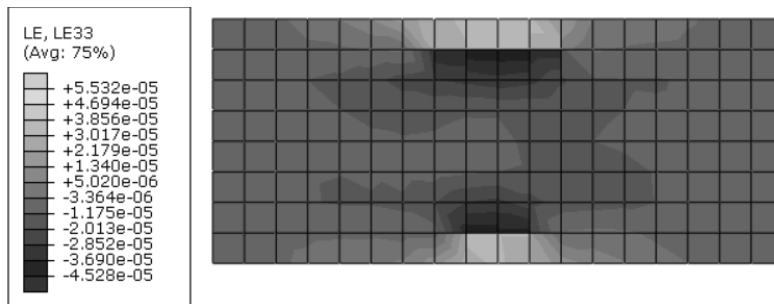


Figure 4. Maximum principal plastic strains (m).

Nodal plastic response (where stress and strain amounts are greater) of one element in the center of the wall was determinate and stress-strain curve for the same element was plotted in the Figure 5.

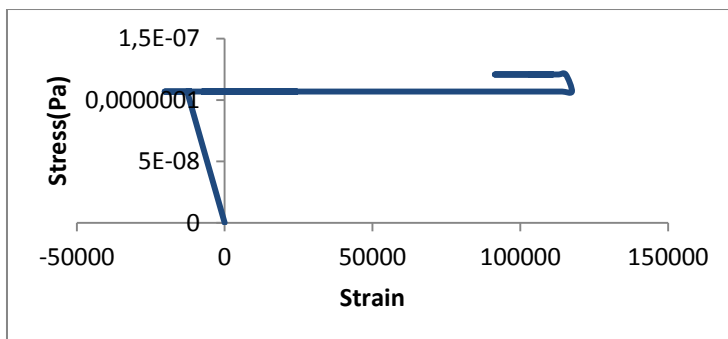


Figure 5. Stress-strain curve of one element in the center of the wall

### 3.2. Model II: RC Column Model

#### 3.2.1. Test Setup

The tested column has 3277 mm of height and cross section of 356 mm x 356 mm with  $\phi$  8 bars as longitudinal reinforcement and  $\phi$  3 bars for circles, spaced at 324 mm from the center and the cover depth is 38 mm. The column was fixed up and bottom, with intense reinforced concrete blocks. A linking system was applied only to the column's head on the side while giving vertical movement, the column was fixed at the base. The experimental model is shown in Figure 6.

The blast load was arterially created using an array of blast generators, each of which was made of impacting module and hydraulic actuator. The maximum equivalent pressure of 19.0 MPa was measured during 0.93 ms after explosion occurred.



Figure 6. Experimental model of the tested column [6]

#### 3.2.2. Numerical Simulation

Since the bottom and heading of the column were confined and heavily reinforced, they were assumed to be linearly elastic in the FE model. The concrete column was modelled using 16224 elements of C3D8R type. The reinforcement bars were modelled using 1372 Timoshenko beam elements (B31) and classic steel plasticity [6] which was embedded in concrete elements. The blast load was simulated using the equivalent pressure measured in the experiment developed by Rodriguez et. al [7]. The explosion was equivalent to 558 kg of TNT material at a distance of 4.36 m. Concrete material properties are the following:  $E_{ci} = 24$  GPa,  $\nu = 0.2$ ,  $f_{cm} = 40$  MPa and  $\rho = 2400$  kg / m<sup>3</sup>. The yield stress of longitudinal bars are:  $f_y = 335$  MPa and circles are equal:  $f_y = 235$  MPa.

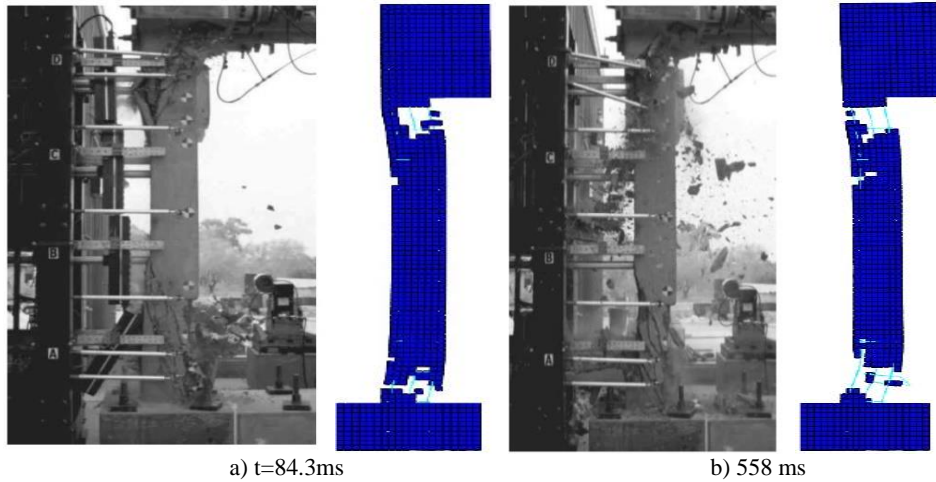
Couple Damage Plasticity model has been used to simulate the column and values of the 5 parameters required are shown in the Table 2.

Table 2. CDP model parameters

$\Psi$	$\epsilon$	$f_{bo} / f_{co}$	$\mu$	$Kc$
38°	0.1	1.16	0.01	0.667

### 3.2.3. Results

The column eventually failed in both test and FE model due to shear failure at its both ends, as shown in the Figure 7. The peak deflection recorded in the experimental model at 41.7 ms was 122 mm, while in the FE model at 43.2 ms was 116.3 mm. The residual deflection recorded in the experiment model was 85 mm, while in the FE model it was 92 mm.



**Figure 7.** Experimental and FE results

At the mid height of the column, both experimental and numerical displacement curves can be observed in the Figure 8. The two curves show a very good similarity, therefore it can be concluded that the numerical analysis closely followed the experimental test and provided an accurate prediction of an evolution of damage and deflections in the column.

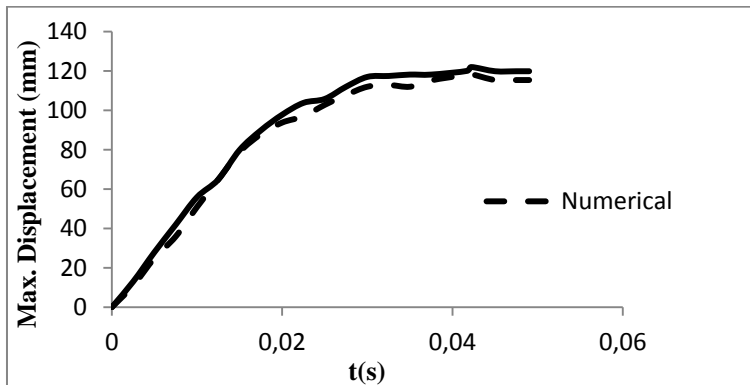


**Figure 8.** Comparison of experimental and numerical displacement

#### 4. MODELING OF RC BUILDING

In this section, the behavior of 6-storey reinforced concrete building with and without infill wall under blast loading has been studied.

Numerical model, for both building were developed using finite element method were cubic 8-node HEX type marked as C3D8R elements, with the following shape function has been used:

$$N_i^e = \frac{1}{8}(1 + \xi\xi_i)(1 + \eta\eta_i)(1 + \mu\mu_i) \quad (6)$$

Were  $\xi_i$ ,  $\eta_i$  and  $\mu_i$  are the natural coordinates of the  $i$  th node.

An explosion of 1000kg TNT weight of a bomb placed in the front face of the building at 4.6m of distance was overloaded. The maximum pressure  $P_{QS} = 35.06$  MPa at the time  $t_k = 25$  ms were determined according to the TNT weights and explosion standoff distance by using the time-dependent pressure function of Newmark approach in terms of determination of wave parameters on the surface of an structure.

Crucial assumptions:

The air medium exceeds any obstacle or charge,

Hemisphere TNT charge has been used,

Obstacles and ground have been assumed as rigid, non-deformable bodies.

##### 4.1. Modeling of RC Building Without Infill Wall

The building has 10.0m × 15.0m of dimensions in longitudinal and transversal direction and 18m of height. Each floor has 3m of height and the structure is composed with frame system. Beam and column have 0.4 x 0.4 m of section and have been spaced with 5 m intervals on both sides, longitudinal and transversal directions.

##### 4.1.1. Numerical Simulation

As defined and described above in the section 3 (modeling of experimental studies), the same properties of materials and method used in the experimental studies developed by Rodriguez et al. [7] were used.

##### 4.1.2. Results

Explosion damage assessment is difficult, knowing that the use of data to drive possible cause and effect relationships and validate with the numerical model, could be very time consuming. However in this numerical model approximation of damage assessment has been determined and results can be observed in Figure 9.

According to the results damage index on the frame structure, in both tensile and compression after the explosion loading can be observed in the Figure 9. It can be notified that the maximum damage which was colored in red starts in the first floor and gets decrease one floor after another floor. Another important observation is that the damage in tensile is greater than the one observed in compression, this can be explain by the fact that the resistance of concrete in tensile is lower.

##### 4.2. Modeling of RC Buiding With Infill Wall

This model consisted in a RC building with same configuration and dimensions as the previous building, but in this case with infill wall which as 25cm of thickness.



### 4.2.1. Numerical Simulation

As defined and described above in the section 3 (modelling of experimental studies), same materials properties and method used in the experimental studies developed by Rodriguez et al. [7], were used for modeling of reinforced concrete. On the other side, same materials properties and method used in the experimental model developed by Pereira et al. [4] have been used to model the masonry structure (infill wall).

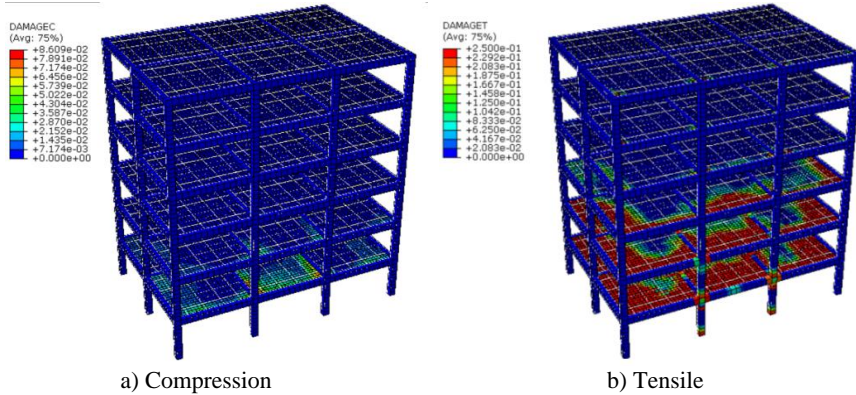


Figure 9. Damage index

### 4.2.2. Results

Here the explosion load applied on the building with infill wall, before its area collapses at any point outside the zones close to the boundary condition, the building reaches the plastic state. Moreover, stress, deformation and energy waves begin to emerge and spread throughout the structure. As observed in the Figure 10, the damage is greater in the first floor before evaluated in the hinges of each floor.

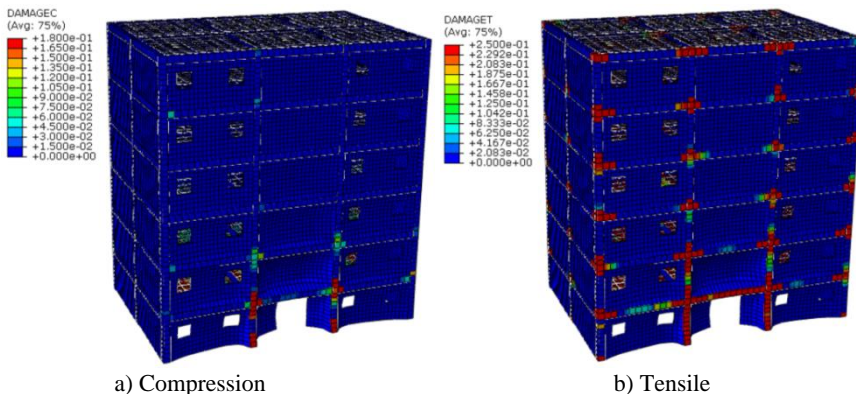
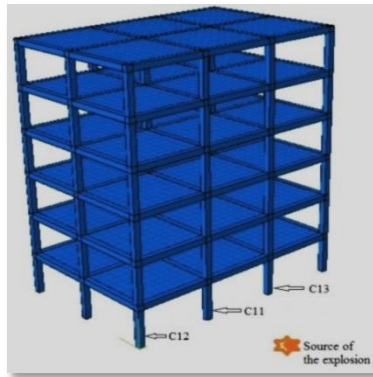


Figure 10. Damage index

## 5. DISCUSSIONS

The dynamic behavior of the building without infill wall and with infill wall, series of comparison have been done by selecting 3 columns at the 1st floor (C11, C12 and C13) as shown in the Figure 11.



**Figure 11.** Reinforced Concrete Building

- Displacement

At mid height of each selected columns, maximum displacement have been determined. It can be observed that for the three columns there is a significant difference between two graphics, in which the maximum value of the nodal displacement is observed in the case of building with infill wall, as shown in the Figures 12-14.

**Column C11**

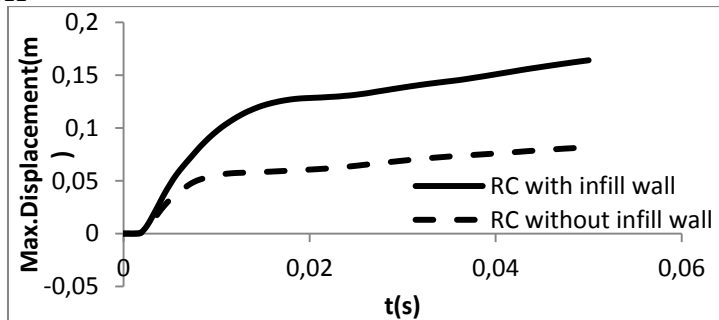


**Figure 12.** Max. Displacement at mid height of C11 column

**Column C12**

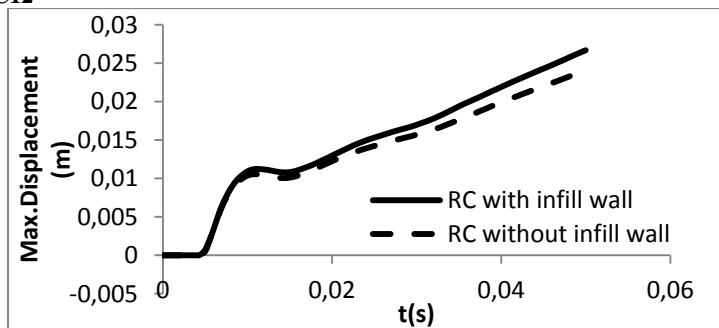


**Figure 13.** Max. Displacement at mid height of C12 column

**Column C13**

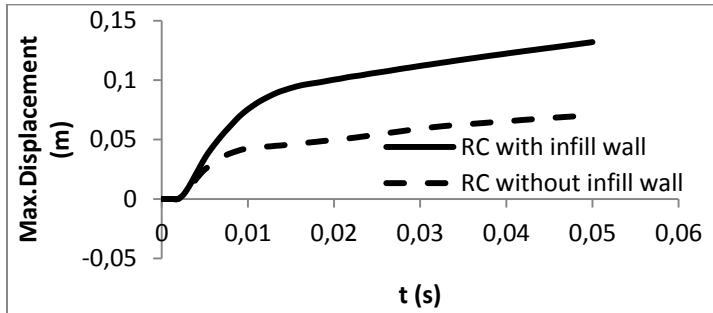


**Figure 14.** Max. Displacement at mid height of C13 column

Also the comparative values of maximum displacement can be observed in the Table 3, as follow:

**Table 3.** Max. Displacement Values

Column	Max. Displacement (m)		Difference
	RC with infill wall	RC without infill wall	
<b>C11</b>	0.164157	0.0817408	0.082416
<b>C12</b>	0.0266865	0.02424	0.002447
<b>C13</b>	0.132003	0.0703641	0.061639

• **Stress**

At the bottom elements of each selected columns, it has been determined the value of stress as shown in the Figures 15-17. The curves generally have the same shapes but the maximum stress values were observed when the building is closed (with infill wall). Approximately there is 11.94% of reduction in term of stress for the column C11, 13% for column C12 and 5.12% for column C13, this can be explained by the fact that after explosion occurred the building without infill wall stored less strain energy, Figure 23.

**Column C11**

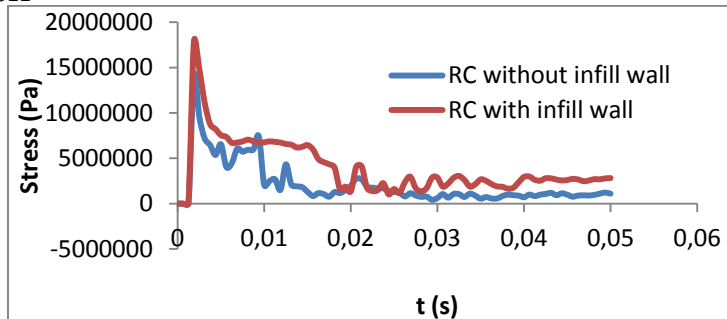


**Figure 15.** Stress at bottom element of the Column C11

**Column C12**

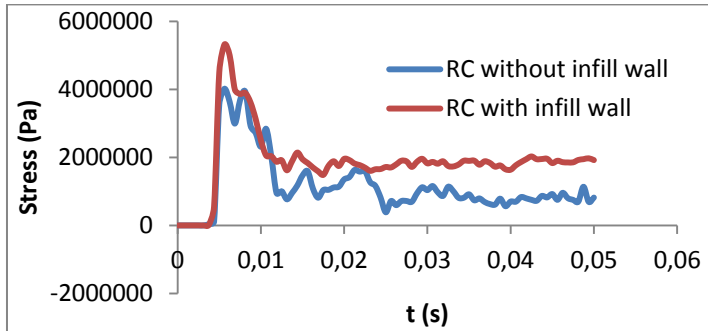


**Figure 16.** Stress at bottom element of the Column C12

**Column C13**

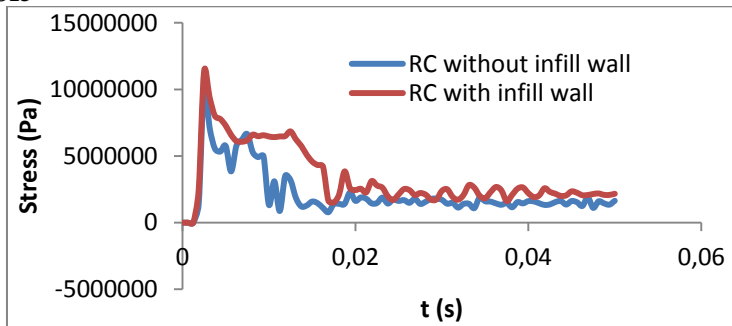


**Figure 17.** Stress at bottom element of the Column C13

- **Deflection**

From the Figures 18-20, the major deflection of the three columns is observed in the case of building with infill Wall.

**Column C11**

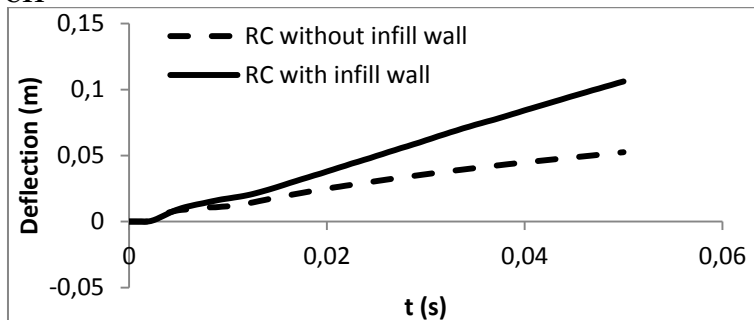


**Figure 18.** Deflection of the Column C11

- **Storey displacement**

It is important to notify that blast load has lateral component, so for structures exposed to high-explosion, floor drift, Figure 21, also needs to be balanced. Knowing that the stability

control of a multi-storey building is defined by storey displacement assessment, which is dimensionless parameter and is given in equation 7. In this study, for both cases analyzed, drift of each floor has determinate.

**Column C12**

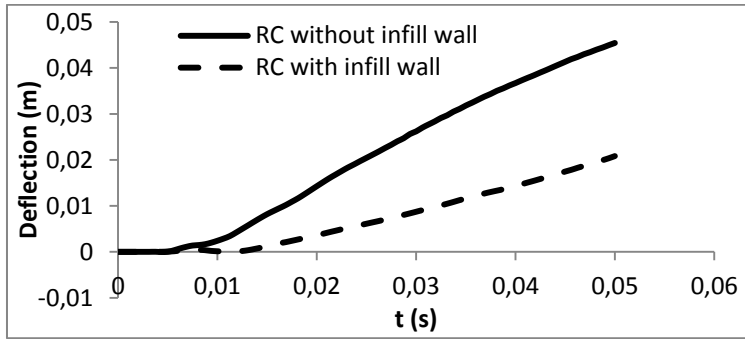


**Figure 19.** Deflection Column C12

**Column C13**

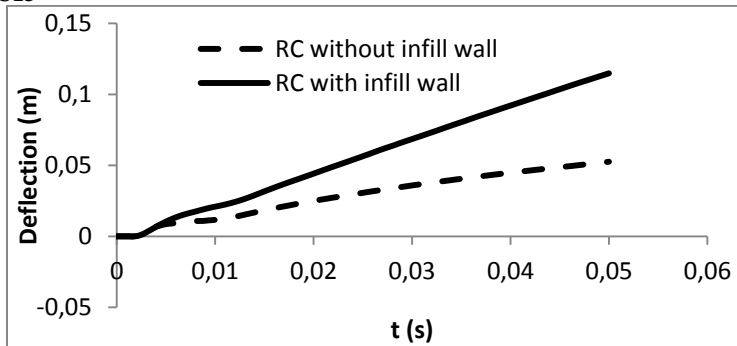


**Figure 20.** Deflection of Column C13

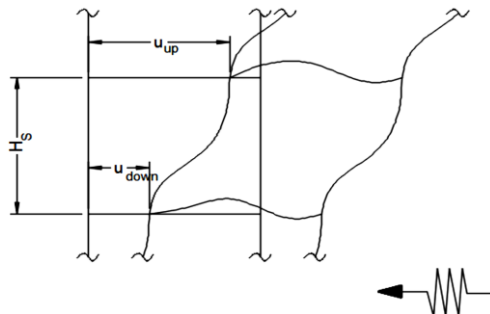


**Figure 21.** Floor drift

$$d_s = \frac{u_{up} - u_{down}}{h_s} \tag{7}$$

Where:

$d_s$  is the floor displacement

$u_{up}$  is the horizontal displacement at the top of up floor

$u_{down}$  is the horizontal displacement under up floor

$h_s$  is the floor height

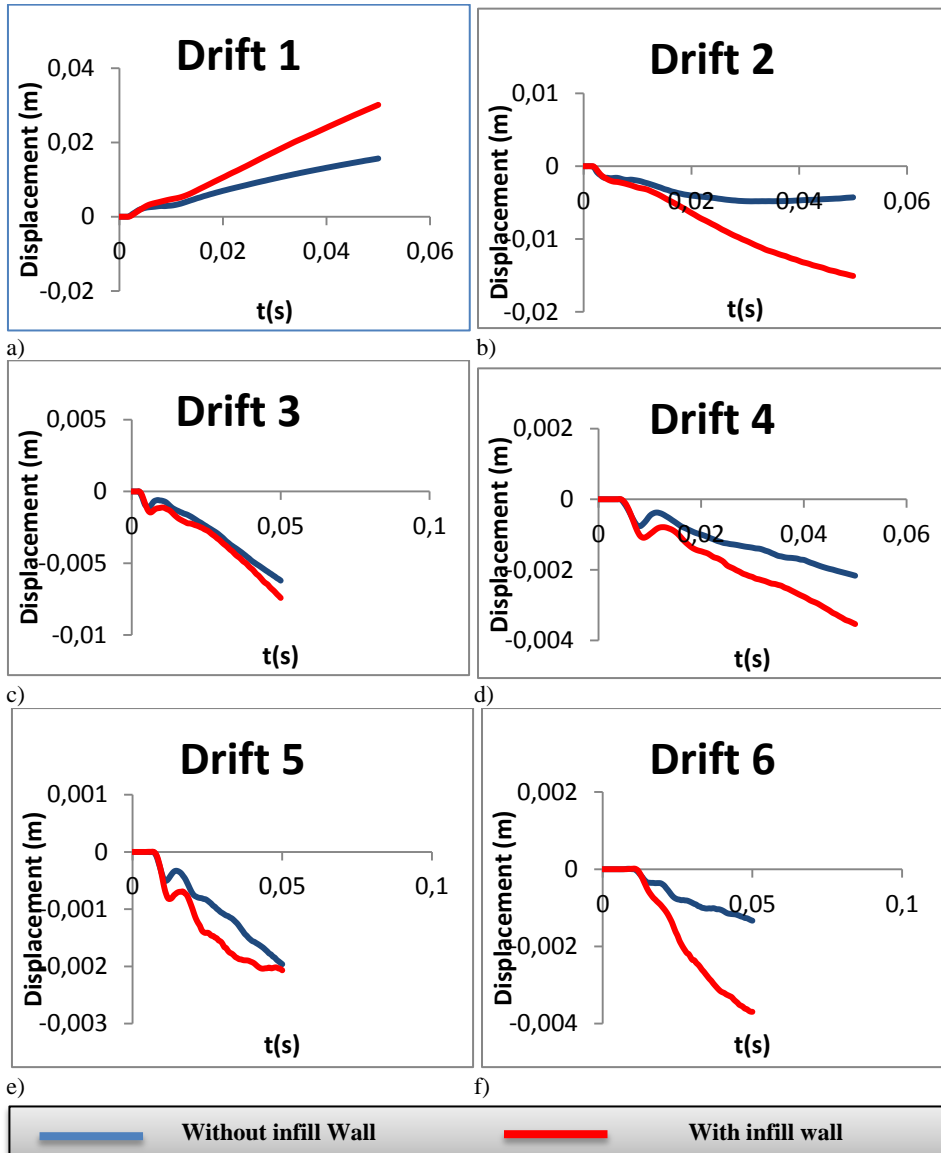


Figure 22. Comparison of storey displacement

According to the results presented in the Figure 22 (a,b,c,d,e and f), the maximum floor drift is observed in the first floor, and values of the first floor are respectively: 15,67 mm for the building without infill wall and 30.13mm for the building with infill Wall

• **Strain Energy**

Energy balance is important for a non-linear FE analysis. Where in static analysis; the total energy should ideally be zero. But in dynamic analysis, the total energy may not necessarily be close to zero, especially for the case of blast loading , knowing that for 1ton of TNT corresponds 4.2 E9 J of total energy. Comparisons between various energy components should be used to evaluate whether an analysis is providing an appropriate response. This is highly required in problem involving significant instabilities. But in this study only the strain energy (0.14E9J) which is equal to the work done by slowly increasing load applied to a member of the structure is determined, Figure 23.

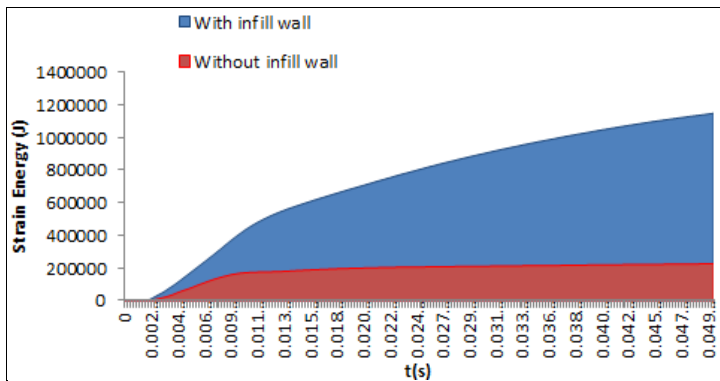


Figure 23. Strain Energy

The nearest column (C11) to the explosion, where the damage is supposed to be greater has been selected and relationship Force-displacement of a nodal element at the mid height of the column has been determined as shown in the Figure 24. The maximum value of the load was observed at the time of impact and started decreasing till the end; however the maximum displacement coincided almost at the minimum value of the applied load.

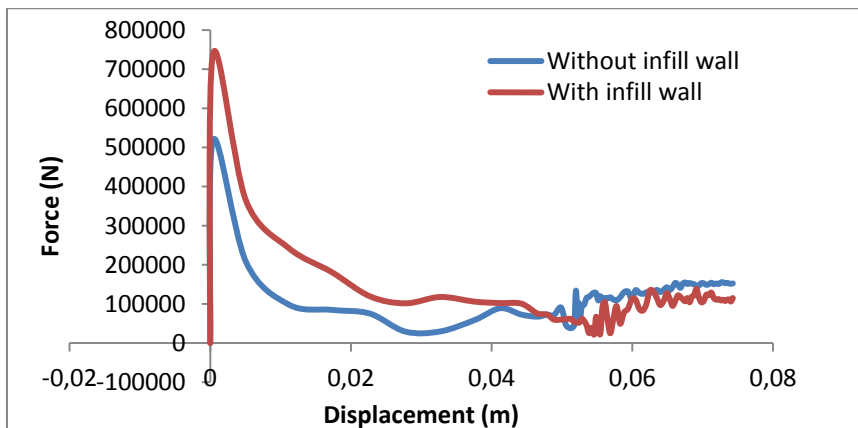


Figure 24. Relationship load-displacement

## **6. CONCLUSION**

A modeling of nonlinear behavior of 6 storey reinforced concrete building without and with infill wall is presented. Coupled Damage Plasticity models are taken into account. They are introduced in a program of analysis for FE method of structures under blast loading. Several physical and numeric parameters are taken into account. It has been concluded that:

- As soon as the explosion load reached the building, in a large majority of the columns and beams, plastic hinges were formed.
- Stress values, deflections, nodal forces, energies and displacements of columns in the RC building with infill wall are higher than those observed in columns belonging to the RC building without infill wall.
- Walls are more vulnerable to the blast effect and the rate of open area in the building reduces the effect of the explosion.
- The drifting of an open structure under blast loading can be neglected, since the building under blast scenario doesn't act as a console. When the weight of the structure is greater, the displacement and deflection of its columns become more significant.
- Depending on the nature of the building and the magnitude of the explosion load, excessive stress, strain and energy fluctuations can be the cause of the building collapse.

## **REFERENCES**

- [1] Feng Fu, (2009). "Advanced Modeling Techniques in Structural Design", Wiley Blackwell, City University London.
- [2] Alex M. Remennikov and Timothy A. Rose (2005), "Modelling blast loads on buildings in Complex city geometries", *Computers & Structures*, 83 (27), 2197-2205.
- [3] A.P. Mouritz, D.S. Saunders, S. Buckley, (1994). "The damage and failure of GRP laminates by underwater explosion shock loading", *Composites* 25 431-437.
- [4] Pereira, M.F.P., Pereira, M.F.N., Ferreira, J.E.D., Lorenzo, P.B.: Behavior of damaged masonry infill panels in RC frames subjected to out of plane loads. In: Proc. of the 7th International Conference on Analytical Models and New Concepts in Concrete and Masonry Structures. Poland 2011.
- [5] Pereira, M.F.P.: Avaliação do desempenho das envolventes dos edifícios face à ação dosismos (in Portuguese). PhD-Thesis, University of Minho, 2013. Department of Civil Engineering: Guimarães 2013.
- [6] Abaqus User Manual, Dassault Systems Simulia Corporation, Providence USA, 2013.
- [7] Rodríguez-Nikl, T. Experimental simulations of explosive loading on structural components reinforced concrete columns with advanced composite jackets, PhD Thesis, University of California, San Diego, 2006, p. 252.